JOURNAL OF MATERIALS SCIENCE **34** (1999) 5669–5675

Multi-strengthening effects on the martensitic transformation temperatures of TiNi shape memory alloys

S. K. WU*
Institute of Materials Science and Engineering, National Taiwan University, Taipei, Taiwan 106, Republic of China
E-mail: skw@ccms.ntu.edu.tw

H. C. LIN
Department of Materials Science, Feng Chia University, Taichung, Taiwan 400, Republic of China

P. C. CHENG
Institute of Materials Science and Engineering, National Taiwan University, Taipei, Taiwan 106, Republic of China

The multi-strengthening effects, introduced by combining cold rolling, aging and thermal cycling, on the martensitic transformation temperatures of $Ti_{50}Ni_{50}$ and $Ti_{49}Ni_{51}$ shape memory alloys have been studied by using DSC and microhardness measurements. Experimental results show that both pre-cold-rolling of $Ti_{50}Ni_{50}$ alloy and aging treatments of $Ti_{49}N_{51}$ alloy can impede the further introduction of dislocations during the thermal cycling and hence effectively reduce the effect of thermal cycling on transformation temperatures. For $Ti_{49}Ni_{51}$ alloy, whether the cold rolling is conducted before or after the aging treatment, the strengthening of cold rolling can significantly increase the specimen hardness but only slightly affect the following thermal cycling effect. The multi-strengthening effects on the martensitic transformation temperatures are also found to follow the equation of $Ms = T_0 - K\Delta\sigma_y$.

1. Introduction

TiNi alloys are known as the most important shape memory alloys (SMAs) because of their many applications based on the shape memory effect (SME) [1] and pseudoelasticity (PE) [2, 3]. This comes from the fact that TiNi alloys have superior properties in ductility, fatigue, recoverable strain, biocompatibility and corrosion resistance. Intensive studies have been made on the transformation behaviors and mechanical properties of TiNi alloys [2–5]. It has been confirmed that TiNi SMAs can be affected by the internal stress retained in the alloys after various thermo-mechanical treatments, such as cold rolling [6–8], thermal cycling [9, 10] and aging treatment in Ni-rich alloys [11–13]. Meanwhile, the properties of SME and PE are reported to be improved by these thermo-mechanical treatments [3, 14]. These treatments can strengthen the alloys and suppress the permanent plastic deformation by raising the flow stress for slip. However, the multi-strengthening effects, introduced by combining these thermo-mechanical treatments, on the martensitic transformations of TiNi alloys have still not been reported. In this study, we combine the processes of cold rolling, thermal cycling and aging to strengthen the TiNi alloys with an aim to understand the multi-strengthening effects on the martensitic transformation temperatures of TiNi alloys.

2. Experimental

The conventional tungsten melting technique was employed to prepare the $Ti_{50}Ni_{50}$ and $Ti_{49}Ni_{51}$ (in at %) alloys. Titanium (purity, 99.8%) and nickel (purity, 99.9%) were melted and remelted at least six times in an argon atmosphere. Pure titanium buttons were also melted and used as getters. The as-melted buttons were homogenized at 1050 °C for 72 h. These buttons were cut into several plates of 3 mm thickness with a low speed diamond saw and then annealed at 800 °C for 2 h and subsequently quenched in water. After annealing, several multi-strengthening treatments, e.g. cold rolling + thermal cycling, aging + cold rolling + thermal cycling, etc. were conducted. The martensitic and R-phase transformation temperatures were measured by using the differential scanning calorimetry (DSC) of Du Pont 2000 thermal analyzer equipped with a quantitative scanning system 910 DSC cell and a cooling accessory

* Author to whom all correspondence should be addressed.

LNCA II. Measurements were carried out at temperatures ranging from −150 to 200 °C under a controlled cooling/heating rate of 10 °C/min. Heats of transformation (ΔH) were automatically calculated from the areas under DSC peaks by means of an equipment software. Specimens for hardness tests were mechanically polished and measured in a microvickers hardness tester at room temperature, with a load of 500 g. For each specimen, the average hardness value was taken from at least five test readings.

3. Results and discussion

3.1. Cold rolling + thermal cycling

Fig. 1a–c show DSC curves of $Ti_{50}Ni_{50}$ specimens with the conditions of as-annealing, 10% cold-rolling at room temperature (cold-rolled at martensite B19′ phase) and 16% cold-rolling at 150 °C (cold-rolled at parent B2 phase), respectively. Fig. 1a represents typical DSC curves of stress-free $Ti_{50}Ni_{50}$ alloy in which the exothermic and endothermic peaks are associated with the B2↔B19′ martensitic transformation. The cooling curve shows the peak temperature M^* near 23.3 °C and the heating curve shows the peak temperature A^* near 69.6 °C. In Fig. 1b, for the specimen with 10% cold-rolling at room temperature, A_1^* temperature appears at 112.9 °C on the first heating cycle of room temperature to +200 °C; M^* temperature appears at 19.3 °C on the following cooling cycle of +200 to −100 °C; and A_2^* temperature appears at 62.7 °C on the second heating cycle of −100 to +200 °C. This phenomenon is referred to as the martensite stabilization induced by the deformed martensite structures of cold-rolled TiNi alloys [8]. After the first reverse martensitic transformation, the martensite stabilization dies out and transformation temperatures are depressed by the retained dislocations on subsequent thermal cycles. In Fig. lc, for the specimen with 16% cold rolling at 150 °C, no transformation peak is observed on the first heating cycle of room temperature to +200 °C; two peaks associated with R-phase and martensitic transformations respectively appear on the following cooling cycle, and a martensitic transformation peak appears during the second heating cycle. This phenomenon can be explained as below. Because the cold-rolling is carried out at 150 °C, i.e., at the parent B2 phase, there should be no deformed martensite structure and hence no martensite stabilization can occur. The retained dislocations induced by cold-rolling at the parent B2 phase will depress the M^* and A^* temperatures and promote the formation of R-phase on the cooling cycle.

Fig. 2a–c show the DSC curves of thermal cycling N = l–100 for the as-annealed, 10% cold-rolled, and 32% cold-rolled (both are cold-rolled at room temperature, i.e., B19′ phase) $Ti_{50}Ni_{50}$ specimens, respectively. In Fig. 2a, the M^* and A^* temperatures are found to decrease significantly with increasing thermal cycles and R-phase transformation appears in the cooling after 10 cycles. These features are well known to be related to the dislocations introduced by thermal cycling. In Fig. 2b, the M^* and A^* temperatures have only a slight decrement during the course of thermal cycling. The R-phase transformation appears just after the second cycle. This means that the pre-cold-rolling can depress the effect of thermal cycling on martensitic transformation temperatures but at the same time promote the R-phase transformation. Here, the R-phase transformation is essentially unaffected by pre-cold-rolling, but since the M^* temperatures are depressed and the R-phase becomes observable. The more the pre-cold-rolling, the less the effect of thermal cycling on transformation temperatures, as shown in Fig. 2c for the 32% pre-cold-rolling specimen. In Fig. 2c, there is no obvious effect of thermal cycling because M^*, A^* and R^* temperatures maintain nearly the same values during thermal cycling. This phenomenon is ascribed to the strengthening dislocations introduced by the pre-cold-rolling. These dislocations will inhibit the further introduction of dislocations during the course of thermal cycling and hence reduce the effect of thermal cycling. Similar phenomenon also occurs on the specimens pre-cold-rolled at the $Ti_{50}Ni_{50}$ B2 parent phase. As shown in Fig. 3a and b, there is only a slight or even nonexistent effect of thermal cycling on transformation temperatures for $Ti_{50}Ni_{50}$ specimens subjected to 7 and 21% pre-cold-rolling at their B2 phase, respectively.

Fig. 4a and b show the specimen hardness as a function of thermal cycles for $Ti_{50}Ni_{50}$ specimens subjected to various degrees of pre-cold-rolling at the martensite and B2 phase, respectively. In Fig. 4a, the hardness of

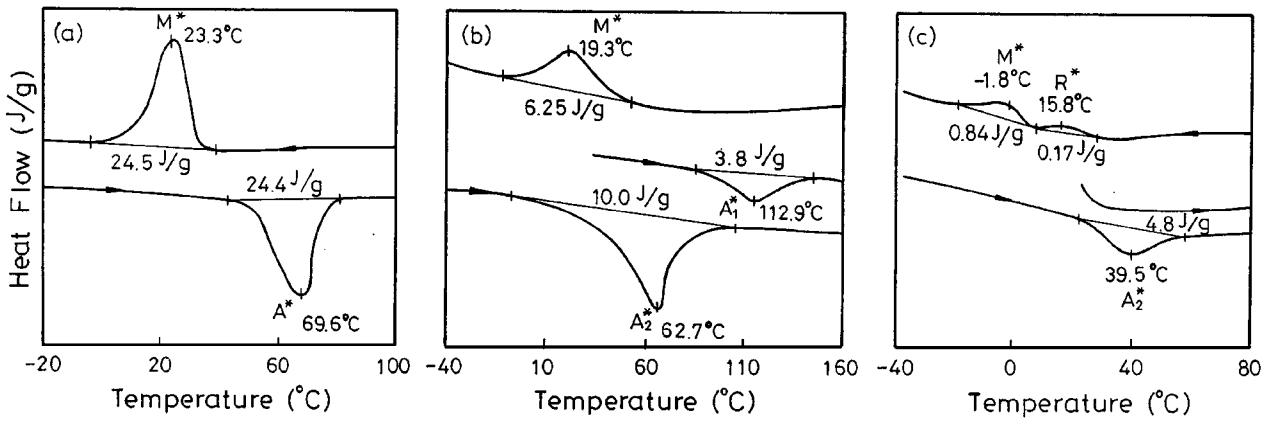

Figure 1 The DSC curves for the $Ti_{50}Ni_{50}$ specimens with the conditions of (a) as-annealing, (b) 10% cold-rolling at martensite B19′ phase, (c) 16% cold-rolling at parent B2 phase.

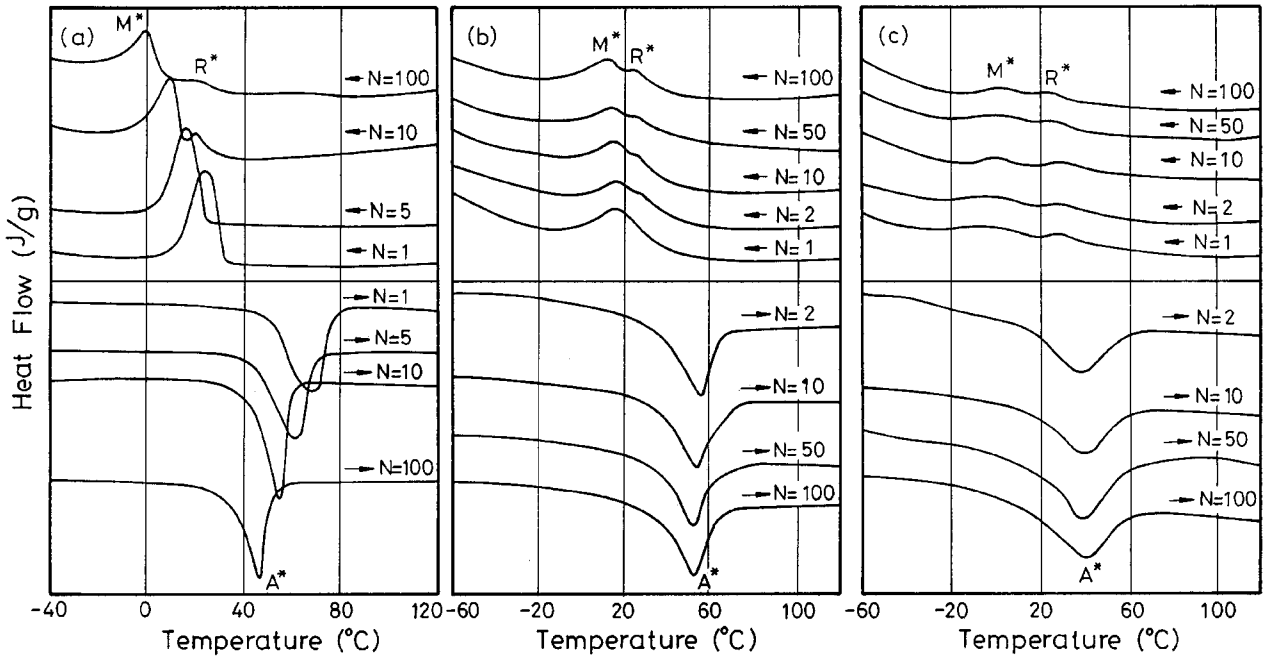

Figure 2 The DSC curves of thermal cycling $N = 1$–100 for the TiNi specimens with the conditions of (a) as-annealing, (b) 10%, (c) 32%. Both (b) and (c) are cold-rolled at martensite B19′ phase.

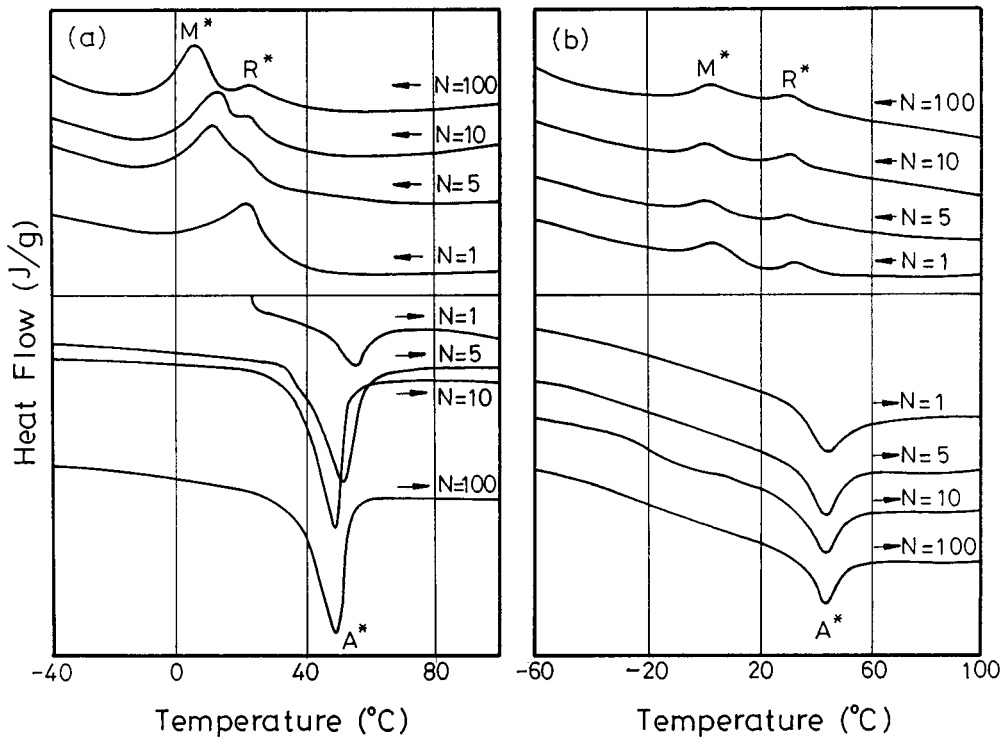

Figure 3 The DSC curves of thermal cycling $N = 1$–100 for the $Ti_{50}Ni_{50}$ specimens subjected to (a) 7%, (b) 21% pre-cold-rolling at parent B2 phase.

as-annealed specimen increases with increasing thermal cycles due to the introduction of dislocations during thermal cycling. However, it is interesting to find that the hardness of 10–32% pre-cold-rolled specimens decreases with increasing cycles in the early thermal cycles and then maintains some constant values after 20 cycles. The defects annihilation of deformed martensite structures and rearrangement of retained dislocations are considered to be responsible for the decrease of specimen hardness in the early 20 cycles. After that, dislocations density and morphology may be unchanged and hence the specimen hardness can maintain some constant value. In Fig. 4b, the hardness of a 7% pre-cold-rolled specimen slightly increases with increasing cycles. This indicates that a few dislocations can be introduced during the course of thermal cycling and hence thermal cycling still has some effect on transformation temperatures, as shown in Fig. 3a. However, for the 16 and 21% pre-cold-rolled specimens, no obvious variation of specimen hardness is observed after 10 cycles in Fig. 4b and hence no obvious effect of thermal cycling can appear. The results of Fig. 4 provide more evidence

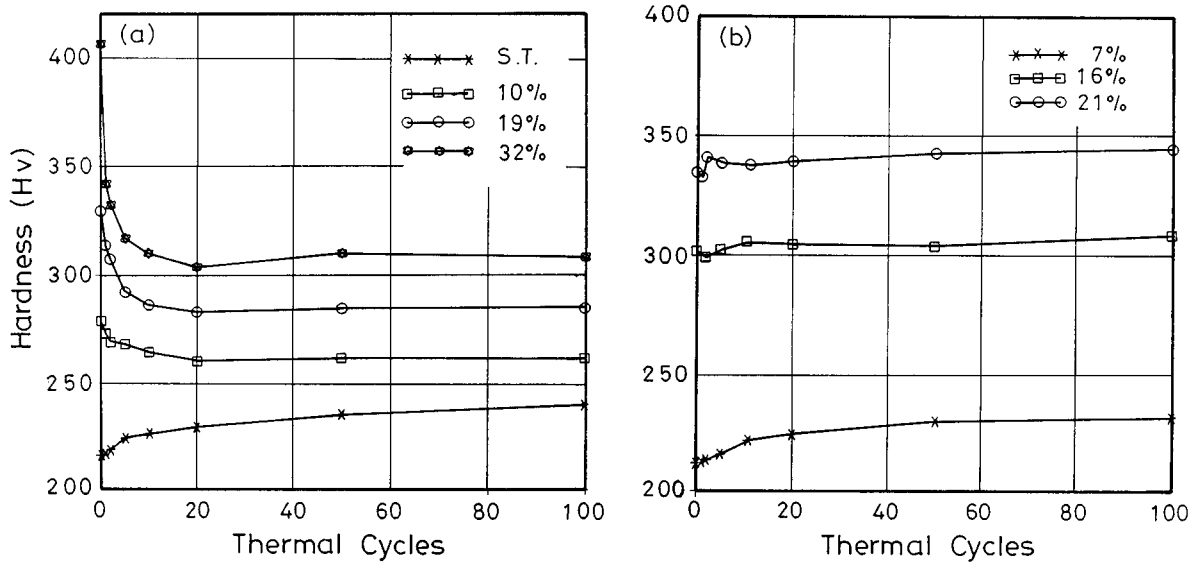

Figure 4 The specimen hardness as a function of thermal cycles for the $Ti_{50}Ni_{50}$ specimens subjected to various degrees of pre-cold-rolling at (a) martensite B19′ phase, (b) parent B2 phase.

to clarify the fact that the effect of thermal cycling can be impeded by pre-cold-rolling. By the way, compared to Fig. 4a, no significant hardness decrement on the early cycles of Fig. 4b can be observed for the pre-cold-rolled specimens because no deformed martensite structure exists in specimens which were subjected to cold-rolling at parent B2 phase.

TABLE II The specimen hardness at various cycles for the 400 °C × 20 h aged $Ti_{49}Ni_{51}$ specimen

Thermal cycle *N*	1	2	5	10	20	50	100
Hardness (Hv)	333.2	332.8	333.6	334.9	332.7	331.6	332.5

3.2. Aging + thermal cycling

It is well known that the martensitic and R-phase transformation temperatures are all affected by the aging time in a 400 °C aged $Ti_{49}Ni_{51}$ alloy. The variation of these transformation temperatures vs. aging time periods is similar to that reported in our previous paper [15]. Table I presents the specimen hardness at various aging time periods for the 400 °C aged $Ti_{49}Ni_{51}$ specimens. From Table I, we can find that the specimen hardness increases rapidly to reach a maximum value at 1–2 h aging and then decreases slowly with further aging. This feature is related to the precipitation hardening of coherent $Ti_{11}Ni_{14}$ precipitates in the TiNi matrix [16]. In order to understand the aging effect on the thermal cycling, the 400 °C × 20 h aged $Ti_{49}Ni_{51}$ specimen is selected to run the thermal cycling. The DSC curves at 1–100 cycles for this specimen are shown in Fig. 5 and the specimen hardness at various cycles are presented in Table II. As can be seen in Fig. 5 and Table II, the transformation temperatures and specimen hardness nearly maintain the same values during the course of thermal cycling. This indicates that the 400 °C × 20 h aged $Ti_{49}Ni_{51}$ specimen shows no obvious effect of thermal

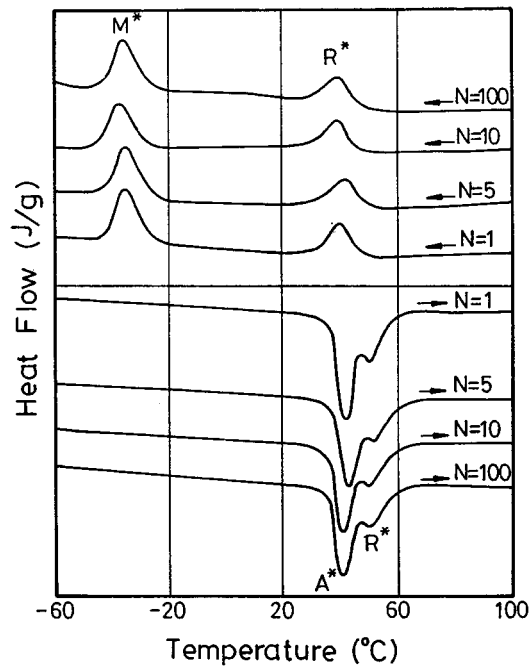

Figure 5 The DSC curves of thermal cycling N = l–100 cycles for the 400 °C × 20 h aged $Ti_{49}Ni_{51}$ specimen.

TABLE I The specimen hardness at various aging times for the 400 °C aged $Ti_{49}Ni_{51}$ specimens

Aging time	As solution — treatment	1 h	2 h	5 h	10 h	20 h	50 h	100 h
Hardness (Hv)	280.3	366.0	366.2	354.0	340.4	333.2	306.8	296.2

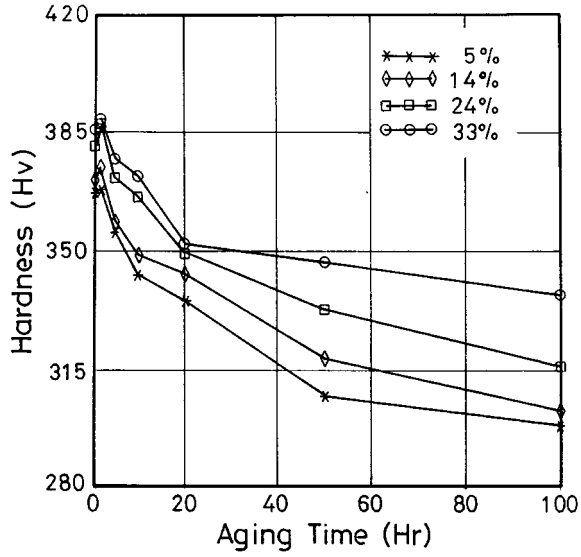

Figure 6 The specimen hardness vs. 400 °C aging time for $Ti_{49}Ni_{51}$ specimens subjected to various degrees of cold-rolling at parent B2 phase.

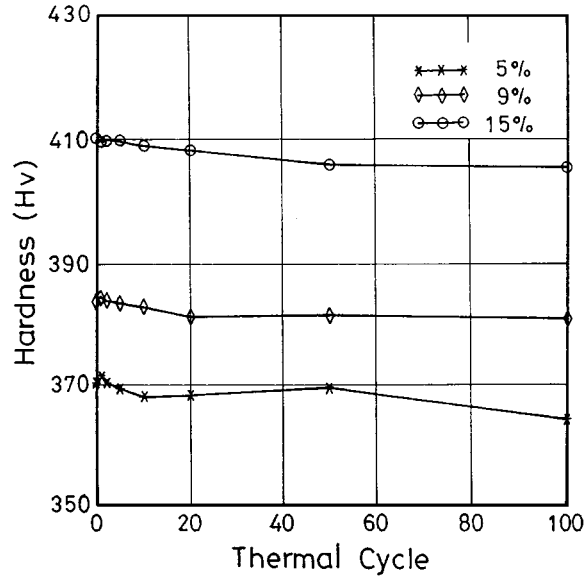

Figure 7 The specimen hardness vs. thermal cycles for the 400 °C × 20 h aged $Ti_{49}Ni_{51}$ specimens subjected to the following 5–15% cold rolling.

cycling. In other words, the dislocation density may not be increased during the thermal cycling for this aging-strengthened $Ti_{49}Ni_{51}$ specimen. In the same way, the 400 °C × 1–20 h aged specimens should exhibit similar phenomenon during the thermal cycling, because they are also strengthened by $Ti_{11}Ni_{14}$ precipitates and their hardnesses, as presented in Table I, are higher than that of the 400 °C × 20 h aged specimen.

3.3. Cold rolling + aging

Fig. 6 shows the variation of specimen hardness as a function of 400 °C aging time for $Ti_{49}Ni_{51}$ specimens subjected to various degrees of cold-rolling at room temperature (at parent B2 phase). In Fig. 6, the specimen hardness is found to slightly increase in the early 2 h of aging and then monotonically decrease with increasing aging time. In this study, both cold-rolling and 400 °C aging have a strengthening effect on the $Ti_{49}Ni_{51}$ specimens. The solution-treated $Ti_{49}Ni_{51}$ specimen has a hardness of Hv = 280 and increases its hardness to values of Hv = 367–386 after the cold-rolling of 5–33%, as shown in the ordinate of Fig. 6. After cold-rolling, the subsequent precipitation hardening of 400 °C × 20 h aging can further increase the specimen hardness, although the recovery of dislocations introduced by cold-rolling may occur during the aging process. As mentioned in Section 3.2, the precipitation hardening can reach its maximum effect at 400 °C × 2 h of aging, and then decreases with increasing aging time period. Therefore, after 2 h of aging, both the decay of precipitation hardening and the recovery of dislocations will soften the cold-rolled specimens, as shown in Fig. 6. The longer the aging time period, the more the softening effect is, and hence the specimen hardness will decrease with increasing aging time.

3.4. Aging + cold rolling + thermal cycling

Following the results of Section 3.3, the multi-strengthening effect of aging + cold rolling + thermal cycling on transformation temperatures of $Ti_{49}Ni_{51}$ alloy is also investigated. A 400 °C × 20 h aged $Ti_{49}Ni_{51}$ specimen is selected to study this effect. Fig. 7 shows the specimen hardness vs. thermal cycles for the $Ti_{49}Ni_{51}$ specimens aged at 400 °C × 20 h with subsequent 5–15% cold rolling. As shown in the ordinate of Fig. 7, the specimen hardness can be raised to higher values by various degrees of cold-rolling, although these specimens have been strengthened by $Ti_{11}Ni_{14}$ precipitation hardening. During the course of thermal cycling, a little softening occurs due to the rearrangement of retained dislocations, but the specimen hardness generally maintains a nearly constant value for each specimen. Meanwhile, the experimental results of DSC measurement do not exhibit any obvious variation of transformation temperatures, as shown in Fig. 8 for the $Ti_{49}Ni_{51}$ specimen aged at 400 °C × 20 h and then cold-rolled at 9%. These results clearly indicate that the processes of aging and cold-rolling can simultaneously strengthen $Ti_{49}Ni_{51}$ specimens and hence strongly depress the effect of thermal cycling.

3.5. Discussion of multi-strengthening effects on TiNi alloys

According to the experimental results presented in Sections 3.1–3.4, all the strengthening treatments, involving thermal cycling, cold rolling and aging, have their individual effects on the martensitic transformation temperatures. These strengthening effects are also consistent with the reported expression [17–20] of

$$Ms = T_0 - K\Delta\sigma_y \quad (1)$$

where the equilibrium temperature T_0 is a function of chemical composition, and the yield stress $\Delta\sigma_y$ is regarded as proportional to the hardness and the constant K represents the activity of strengthening effects. From Figs 2–4, the K values are found to be 1.19 and

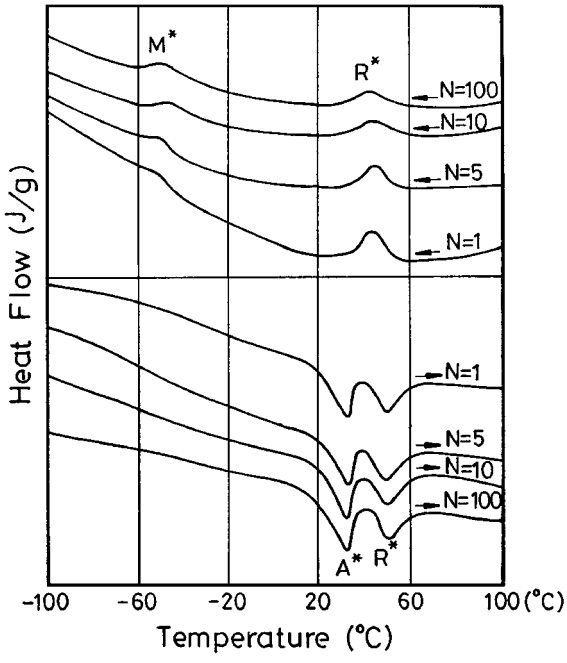

Figure 8 The DSC curves of thermal cycling $N = 1$–100 for the 400 °C × 20 h aged and then 9% cold-rolled $Ti_{49}N_{51}$ specimen.

0.28 °C Hv^{-1} for the strengthening process of thermal cycling and that of cold rolling at the parent B2 phase, respectively. This feature is a result of the different dislocation distribution and/or clustering manner which can be induced by different strengthening processes, because the former strengthening process originates from the B2↔B19′ transformation and the latter one results from the plastic deformation of the B2 phase. The fact that $K = 1.19\,^{\circ}\mathrm{C\,Hv^{-1}} \gg K = 0.28\,^{\circ}\mathrm{C\,Hv^{-1}}$ also indicates that the martensitic transformation temperatures of $Ti_{50}Ni_{50}$ alloy can be more effectively depressed by thermal cycling than by cold rolling at the B2 phase.

From Figs 5–8, the aging treatment for $Ti_{49}Ni_{51}$ alloy can significantly impede the effect of thermal cycling on the transformation temperatures. The cold rolling process, whether it is conducted before (Fig. 7) or after (Fig. 6) the aging treatment, can effectively increase the specimen hardness, but only slightly affects the subsequent thermal cycling effect. This implies that, for $Ti_{49}Ni_{51}$ nickel-rich alloy, the aging precipitation hardening provides a more effective method than cold rolling does to reduce the thermal cycling effect in applications. Meanwhile, it is worthy to mention that although aging can have a strong strengthening effect, it also embrittles the $Ti_{49}Ni_{51}$ specimen. For the 400 °C × 20 h aged $Ti_{49}Ni_{51}$ specimen, brittle fracture may occur sometimes even under 5% cold-rolling and there are lots of microcracks distributed on the fractured surface, as shown in Fig. 9. Therefore, the cold rolling process for the aged $Ti_{49}Ni_{51}$ specimens should be conducted more carefully.

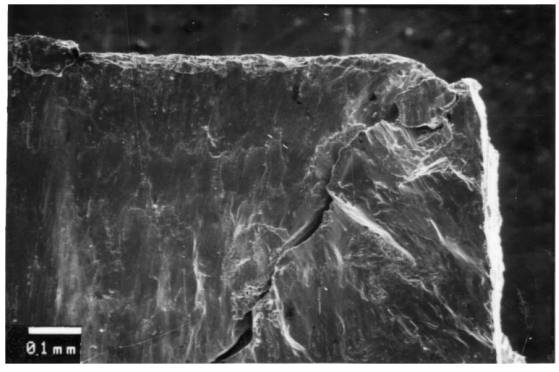

Figure 9 The SEM observation of cold-rolled fracture surface for the 400 °C × 20 h aged $Ti_{49}Ni_{51}$ specimen.

4. Conclusions

The multi-strengthening processes in $Ti_{50}Ni_{50}$ and $Ti_{49}Ni_{51}$ alloys by combining the cold rolling, aging and thermal cycling have significant effects on the martensitic transformation temperatures. Both pre-cold-rolling on $Ti_{50}Ni_{50}$ alloy and aging treatments on $Ti_{49}Ni_{51}$ alloy can impede the further introduction of dislocations during the thermal cycling and hence significantly reduce the effect of thermal cycling. The precipitation hardening of 400 °C × 1–2 h aging treatment can further increase the specimen hardness of pre-cold-rolled $Ti_{49}Ni_{51}$ alloy. On the other hand, the specimen hardness of aging-strengthened $Ti_{49}Ni_{51}$ alloy can also be raised to higher values by the subsequent cold-rolling. However, for $Ti_{49}Ni_{51}$ alloy, whether the cold rolling is conducted before or after the aging treatment, the strengthening of cold rolling has only a slight effect on the following thermal cycling effect. This means that, for $Ti_{49}Ni_{51}$ alloy, the aging process provides an effective method to reduce the thermal cycling effect in SMAs applications. In this study, the multi-strengthening effects on the martensitic transformation temperatures are also found to follow the equation of $Ms = T_0 - K\Delta\sigma_y$.

Acknowledgement

The authors are pleased to acknowledge the financial support of this research by National Science Council (NSC), Republic of China, under Grant NSC 83-0405-E002-011.

References

1. S. MIYAZAKI, K. OTSUKA and Y. SUZUKI, *Scripta Metall.* **15** (1981) 287.
2. S. MIYAZAKI, Y. OHMI, K. OTSUKA and Y. SUZUKI, in Proc. of ICOMAT-82, International Conf. on Martensitic Transformations, Belgium, Supplement to *J. de Physique* **43** (1982) C4-255.
3. S. MIYAZAKI, T. IMAI, Y. IGO and K. OTSUKA, *Metall. Trans. A* **17A** (1986) 115.
4. G. D. SANDROCK, A. J. PERKINS and R. F. HEHEMANN, *ibid.* **2** (1971) 2769.
5. H. C. LING and R. KAPLOW, *ibid.* **12** (1981) 2101.
6. Y. OKAMOTO, H. HAMANAKA, F. MIURA, H. TAMURA and H. HORIKAWA, *Scripta Metall.* **22** (1988) 517.
7. T. TODOROKI and H. TAMURA, *Trans. JIM* **28** (1987) 83.
8. H. C. LIN, S. K. WU, T. S. CHOU and H. P. KAO, *Acta Metall. Mater.* **39** (1991) 2069.
9. T. TADAKI, Y. NAKATA and K. SHIMIZU, *Trans. JIM* **28** (1987) 883.
10. S. MIYAZAKI, Y. IGO and K. OTSUKA, *Acta Metall.* **34** (1986) 2045.

11. M. NISHIDA and T. HONMA, *Scripta Metall.* **18** (1984) 1293 & 1389.
12. S. K. WU, H. C. LIN and T. S. CHOU, *Acta Metall. Mater.* **38** (1990) 95.
13. S. K. WU and H. C. LIN, *Scripta Metall.* **25** (1991) 1295.
14. H. C. LIN and S. K. WU, *Scripta Metall. Mater.* **26** (1992) 59.
15. S. K. WU, H. C. LIN and T. S. CHOU, *Scripta Metall.* **23** (1989) 2043.
16. S. K. WU and H. C. LIN, *ibid.* **25** (1991) 1529.
17. M. COHEN, E. S. MACHLIN and V. G. PARANJPE, "Thermodynamics in Physical Metallurgy" (American Society for Metals, Metals Park, OH, USA, 1950), p. 242.
18. E. HOMBOGEN, *Acta Metall.* **33** (1985) 595.
19. S. EUCKEN and E. HOMBOGEN, *J. Mater. Sci.* **19** (1984) 1343.
20. H. C. LIN and S. K. WU, *Mater. Sci. Eng.* **A158** (1992) 87.

Received 18 November 1996
and accepted 16 April 1999